Experimental Validation of Inverse Techniques for the Remote Identification of Impact Forces in Gap-Supported Systems Subjected to Local and Flow Turbulence Excitations

Xavier Delaune
e-mail: xavier.delaune@cea.fr

Philippe Piteau

Laboratoire d'Etudes de Dynamique,
Commissariat à l'Energie Atomique et aux Energies Alternatives,
CEA, DEN, DM2S, SEMT,
F-91191 Gif-sur-Yvette, France

Vincent Debut

Jose Antunes

Applied Dynamics Laboratory,
Instituto Tecnologico e Nuclear,
ITN/ADL, 2686 Sacavem, Portugal

Predictive computations of the nonlinear dynamical responses of gap-supported tubes subjected to flow excitation have been the subject of active research. Nevertheless, experimental results are still necessary for validation of the theoretical predictions as well as for asserting the integrity of field components. Because carefully instrumented test tubes and tube-supports are seldom possible, due to space limitations and to the severe environment conditions, there is a need for robust techniques capable of extracting relevant information from the actual vibratory response data. Although at the present time such analysis is overambitious, as far as the multisupported tube bundles of real-life components are concerned, the same instrumentation difficulties frequently apply in the case of laboratory test rigs. Therefore, the subject of this paper is of practical significance even in the more modest realm of laboratory experiments. The knowledge of the dynamical contact/impact (vibro-impact) forces is of paramount significance, and also the tube/support gaps. Following our previous studies in this area using wave-propagation techniques (De Araújo et al., 1998; Antunes et al., 1998; Paulino et al., 1999), we recently applied modal methods for extracting such information. Based on numerically simulated time-domain vibro-impact responses, the dynamical support forces, as well as the vibratory responses at the support locations, were identified from one or several vibratory responses at remote locations, from which the support gaps could also be inferred (Delaune et al., 2010). Also recently, for the related problem of friction force identification on bowed strings, preliminary experiments have shown the feasibility of these identification techniques (Debut et al., 2010). In the present paper, the modal identification techniques developed by Delaune et al. (2010) and Debut et al. (2010) are tested using an experimental rig built at Commissariat à l'Energie Atomique et aux Energies Alternatives (CEA/Saclay), consisting of a randomly excited clamped-free beam which impacts on an intermediate gap-support. Identification of the impact force, as well as of the beam motion at the gap-support, is achieved based on remote measurements of the beam response provided by two accelerometers. A significant feature of the experimental identifications presented in this paper is that, beyond the results obtained under a point-force shaker excitation, we test here an original technique to identify the gap-supported reactions in flow-excited systems, which was recently introduced by Delaune et al. (2010). As for most inverse problems, the identification results may prove sensitive to both noise and modeling errors. Therefore, regularization techniques discussed by Delaune et al. (2010) are used to mitigate the effects of unmeasured noise perturbations. Overall, the experimentally identified results compare reasonably well with the measured contact forces and motions at the gap-supports. Actually, even if our identifications are not immaculate at the present time, they remain nevertheless quite usable. [DOI: 10.1115/1.4002926]

1 Introduction

Flow-induced vibrations of heat-exchanger tube bundles and nuclear fuel rods are a major source of concern, when component life and plant availability are addressed. Excitation by the flow turbulence and possible fluid-elastic phenomena may lead to a premature failure of the components due to material fatigue or to vibro-impact wear of the gap-supported tubes. Hence, the authors and other researchers have developed predictive methods and computer codes to analyze heat-exchanger tube responses and wear, for realistic multisupported tubes and flow configurations, with considerable success [1–7], as attested by validation of the predictive techniques achieved through laboratory experiments [8–11].

Laboratory work on vibro-impacting tubes involves carefully instrumented test tubes and tube-supports, see, for instance, Ref. [12]. Such experimental conditions are seldom possible for real

Contributed by the Pressure Vessel and Piping Division of ASME for publication in the JOURNAL OF PRESSURE VESSEL TECHNOLOGY. Manuscript received April 16, 2010; final manuscript received August 31, 2010; published online July 11, 2011. Assoc. Editor: Samir Ziada.

field components, due to space limitations and to the severe environment conditions (temperature and radiation) that prevent an adequate instrumentation of the tube-supports. Therefore, typically, the tube/support impact forces cannot be directly monitored under real operating conditions. Identification techniques that enable the diagnosis of tube/support interaction, based on remote vibratory measurements, are therefore quite valuable, for validating the predictive methods, as well as for condition-monitoring of the real components.

Previous work in this field include papers by Whiston [13] and Jordan and Whiston [14], who discussed theoretical and experimental aspects related to the remote identification of impact forces. These authors modeled the flexural propagation waves in the frequency domain using a Timoshenko beam model without damping. In his book and in a series of related papers, Doyle [15] followed a similar approach. These authors also presented satisfactory experimental results provided by single impacts acting on long beams, in such a way that wave reflections at the boundaries do not interfere seriously with the direct wave used for identification proposes. In a series of papers [16–18], using small arrays of motion transducers, the present authors further extended wave-propagation techniques, based on a simple Bernoulli–Euler beam formulation, in order to deal effectively with the wave reflections arising at the boundary conditions of finite-length beams.

Lin and Bapat [19,20] presented methods for estimating the impact forces and the support gap in a single-degree-of-freedom system, respectively, for sinusoidal and random excitations. The extension of these methods to a beam with a single nonlinear gap-support was proposed by using a modal approach in the frequency domain [21]. Busby and Trujillo [22] presented a similar approach, in which the force identification is achieved in the time domain. Further extension of these methods to multisupported beams, which display ill-defined or even unknown modal basis, seems problematic. Nevertheless, our experimental work [18] performed on a beam with three gap-supports that provided high quality force identifications, provided that vibro-impacts arise at all intermediate gap-supports (e.g., with no preload effects at intermediate supports). Wu and Yeh [23] discussed the problem of source separation, for several simultaneous impacts, using a time-domain approach. The so-called cepstral methods of deconvolution, which may be quite useful when dealing with nondispersive phenomena, have been used very seldom for dispersive flexural waves [24]. The same can be said about the application of the so-called "blind identification" methods to vibro-impact problems, although interesting pioneer results may be found in Ref. [25].

Most of the basic work on inverse theory was triggered by identification problems in the geophysics/astrophysics, radar/sonar, and medical research fields. These problems usually involve nondispersive phenomena, and lead to problems somewhat different from those of concern here. Nevertheless, for an approach to inverse problems, useful information will be found in the applied work by Jeffrey and Rosner [26], Dimri [27], and Parker [28]. In a more general context, Press et al. [29], Groetch [30], Hansen [31], and Grech et al. [32] offered excellent reviews on inverse problems and current methods for solving them.

The main difficulty with inverse problems is ill-conditioning, physical or numerical, of the transfer/propagation operators which describe the phenomena. This leads to inverse formulations that are very sensitive to noise contamination of the measured signals. Problems may be partially overcome by regularization of the transformation operators, by using several methods, namely, singular value decomposition (SVD), incorporation of physical constraints, and optimization techniques [16,29–33]. Another possible source of difficulties lays in the imperfect knowledge of the system parameters used when formulating the inverse problem, the modal frequencies being particularly sensible parameters. This problem is discussed in Ref. [34], where an alleviating approach is proposed and experimentally validated.

The present paper follows our previous work on remote vibro-impact identification using wave-propagation techniques [16–18]. Here, we explore the use of modal techniques for extracting, from one or several vibratory response measurements at remote locations, the dynamical support forces as well as the vibratory responses at the support locations, from which the support gaps may be inferred. Both techniques work in the frequency domain. In contrast to the wave-propagation approach, the modal approach asks for a larger number of parameters in order to describe the system dynamics matrices $H(\omega)$ to be inverted, which is certainly a disadvantage. Indeed, while only a couple of parameters related to the wave speed and dissipation is needed to describe propagation in the $k(\omega)$ dispersion equation, the modal approach needs all the modal parameters m_n, ω_n, ζ_n, and $\varphi_n(x)$, $n=1,2,\ldots,N$ in the frequency range of interest. However, wave-propagation techniques must cope with a multitude of reflected waves stemming from the boundary conditions of finite-length beams, while these effects are automatically encapsulated in the modal parameters, a fact that significantly favors identification techniques based on the modal formulation.

First, experimental identifications of vibro-impact forces are presented in this paper, which were obtained under point-force shaker excitations. However, the most significant feature among the results presented is that we also validate here a simple original technique, recently introduced in Ref. [33], to improve the identification of contact forces at the supports of a flow-excited system, which is subjected to an unknown distributed turbulence force field. Such approach should prove valuable in many instances, particularly, when addressing the difficult problem of identifying nonimpulsive contact forces at preloaded intermediate supports.

The experimental force and gap identifications presented are based on the modal parameters of our test rig, which were identified in preliminary tests. We confront the identified dynamical support contact forces and vibratory motions at the gap-support with the actual values measured using local transducers. Regularization techniques discussed in Ref. [33] are used to mitigate the effects of unmeasured noise perturbations. Overall, the experimentally identified results compare reasonably well with the measured contact forces and motions at the gap-supports. We believe that, even if our present identification results can possibly be improved, they appear already to be quite usable.

2 Basic Identification Problem

The vibro-impact problems addressed in this paper are severely nonlinear. However, one should notice that, if the nonlinear system dynamical responses are known from measurements, then the *inverse problem* of identifying the excitations (including all nonlinear interaction forces) from the available responses becomes *linear*, because the basic unconstrained vibrating system may be modeled as such. In other words, once the system response is available, then even the motion-dependent forces (such as impacts) can be seen as common *external excitations* which led to the measured tube responses. Note that this is true whatever the nature of the nonlinear local forces to be identified. For instance, the dynamical reaction from a support with cubic nonlinearity might be identified using the same approach as the gap-support force identification addressed in this paper.

Then, as discussed in Refs. [33,34], identification of the excitation forces becomes essentially a problem of response deconvolution, when working in the time domain, or, which is more practical, response inversion, by working in the frequency domain. A basic procedure for the identification of excitations $\{f(x_e,t)\}(e=1,2,\ldots,E)$ from the response measurements $\{y(x_r,t)\}(r=1,2,\ldots,R)$ can be summarized as shown in Fig. 1.

Here $[H]^+$ stands for the *pseudo-inverse* of matrix $[H]$, which is built from the following transfer functions:

$$\{y(x_r,t)\} \overset{\mathcal{F}[\ldots]}{\Rightarrow} \{Y(x_r,\omega)\} = [H(x_e,x_r,\omega)]\{F(x_e,\omega)\}$$

$$\Downarrow$$

$$\{F(x_e,\omega)\} = [H(x_e,x_r,\omega)]^{+}\{Y(x_r,\omega)\} \overset{\mathcal{F}^{-1}[\ldots]}{\Rightarrow} \{f(x_E,t)\}$$

Fig. 1 Procedure for sources identification

$$H^D(x_e,x_r,\omega) = \sum_{n=1}^{N} \frac{\varphi_n(x_e)\varphi_n(x_r)}{m_n[\omega_n^2 - \omega^2 + 2i\omega\omega_n\zeta_n]} \quad \text{with} \quad \begin{cases} e = 1,2,\ldots,E \\ r = 1,2,\ldots,R \end{cases} \tag{1}$$

in the case of displacement response measurements. If velocity or acceleration responses are used, then

$$H^V(x_e,x_r,\omega) = i\omega H^D(x_e,x_r,\omega) \tag{2}$$

$$H^A(x_e,x_r,\omega) = -\omega^2 H^D(x_e,x_r,\omega) \tag{3}$$

For systems with more than one excitation and more than one response measurement, the inverse problem must be determinate ($R \geq E$), or else additional information constraints on the interaction forces should be available and included in the formulation. Excitations $e=1,2,\ldots,E$ include both the actual energy sources (electromagnetic shakers and flow force field), as well as the contact forces at the gap-supports. In order to highlight the different physical nature of these terms, they will be written in the following using the notation:

contact/impact forces: $\{f(x_c,t)\}(c=1,2,\ldots,C)$
shaker excitation: $\{f(x_s,t)\}(s=1,2,\ldots,S)$
distributed flow turbulence excitation: $f_T(x,t)$

Also notice that the modes used when building the transfer functions (1)–(3) are those of the system *unconstrained* at the locations where identifications are to be performed.

Figure 2 shows a sketch of the experimental system, which will be addressed in this paper, consisting on a clamped-free beam with length L with a single gap-support at location x_c. Excitation is provided either (a) by a single electromagnetic shaker at location x_s, or (b) by the turbulence of a transverse flow. These two cases will be next formulated in detail, following Ref. [33].

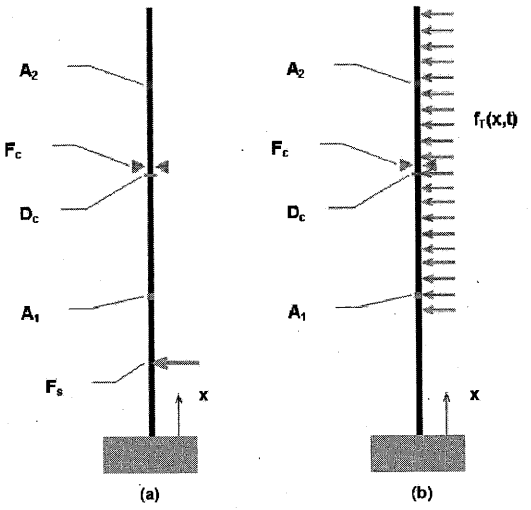

Fig. 2 Experimental vibro-impact system. (*a*) Point-excitation by a shaker and (*b*) distributed flow turbulence excitation.

3 Excitation by a Point-Force

For the system configuration shown in Fig. 2(*a*), the vibratory responses $A_1(t) \equiv A(x_1,t)$ and $A_2(t) \equiv A(x_2,t)$ measured by the accelerometers are due to impact and shaker excitation forces, respectively, $f_c(t) \equiv f(x_c,t)$ and $f_s(t) \equiv f(x_s,t)$. Because the (unconstrained) beam is assumed linear, each vibratory response is given simply by the superposition of the responses to the two excitation terms (whatever their possible correlation). In the frequency domain this reads

$$A_1(\omega) = H^A(x_c,x_1,\omega)F_c(\omega) + H^A(x_s,x_1,\omega)F_s(\omega)$$

$$A_2(\omega) = H^A(x_c,x_2,\omega)F_c(\omega) + H^A(x_s,x_2,\omega)F_s(\omega) \tag{4}$$

which, by inversion, enables the identification of both excitation sources

$$\begin{Bmatrix} F_c(\omega) \\ F_s(\omega) \end{Bmatrix} = \begin{bmatrix} H^A(x_c,x_1,\omega) & H^A(x_s,x_1,\omega) \\ H^A(x_c,x_2,\omega) & H^A(x_s,x_2,\omega) \end{bmatrix}^{-1} \begin{Bmatrix} A_1(\omega) \\ A_2(\omega) \end{Bmatrix} \tag{5}$$

where

$$H^A(x_c,x_r,\omega) = -\omega^2 \sum_{n=1}^{N} \frac{\varphi_n(x_c)\varphi_n(x_r)}{m_n[\omega_n^2 - \omega^2 + 2i\omega\omega_n\zeta_n]} \tag{6}$$

$$H^A(x_s,x_r,\omega) = -\omega^2 \sum_{n=1}^{N} \frac{\varphi_n(x_s)\varphi_n(x_r)}{m_n[\omega_n^2 - \omega^2 + 2i\omega\omega_n\zeta_n]} \tag{7}$$

Notice that, once the excitation forces $F_c(\omega)$ and $F_s(\omega)$ have been identified through Eq. (5), it becomes easy to also identify the displacement $Y_c(\omega)$ at the gap-support:

$$Y_c(\omega) = H^D(x_c,x_c,\omega)F_c(\omega) + H^D(x_s,x_c,\omega)F_s(\omega) \tag{8}$$

4 Excitation by the Flow Turbulence

Now, concerning the system configuration shown in Fig. 2(*b*), a perturbing effect comes from the *distributed* turbulence force field $f_T(x,t)$. In order to try to somewhat correct the degrading effects of the unmeasured turbulence excitation, notice that, if the random excitation was applied at a single point x_T, we would have the following responses:

$$A_1(\omega) = H^A(x_c,x_1,\omega)F_c(\omega) + H^A(x_T,x_1,\omega)F_T(\omega)$$

$$A_2(\omega) = H^A(x_c,x_2,\omega)F_c(\omega) + H^A(x_T,x_2,\omega)F_T(\omega) \tag{9}$$

which would enable the identification of both excitation sources

$$\begin{Bmatrix} F_c(\omega) \\ F_T(\omega) \end{Bmatrix} = \begin{bmatrix} H^A(x_c,x_1,\omega) & H^A(x_T,x_1,\omega) \\ H^A(x_c,x_2,\omega) & H^A(x_T,x_2,\omega) \end{bmatrix}^{-1} \begin{Bmatrix} A_1(\omega) \\ A_2(\omega) \end{Bmatrix} \tag{10}$$

However, the problem is obviously not so immediate, because the turbulence excitation is distributed along the tube in a complex manner, and no transfer functions $H(x_T,x_r,\omega)$ can be defined. Even so, for the distributed random excitation, we may correctly write the response equations as follows:

$$A_1(\omega) = H^A(x_c,x_1,\omega)F_c(\omega) + \sum_{n=1}^{N} \frac{F_n^T(\omega)\varphi_n(x_1)}{m_n[\omega_n^2 - \omega^2 + 2i\omega\omega_n\zeta_n]} \tag{11}$$

$$A_2(\omega) = H^A(x_c,x_2,\omega)F_c(\omega) + \sum_{n=1}^{N} \frac{F_n^T(\omega)\varphi_n(x_2)}{m_n[\omega_n^2 - \omega^2 + 2i\omega\omega_n\zeta_n]} \tag{12}$$

where $F_n^T(\omega)$ stands for the Fourier transform of the modal forces related to turbulence $f_n^T(t)$.

Now, the correct equations (11) and (12) are quite different from Eq. (9). However, it is tempting to simplify this formulation in the following manner:

$$A_1(\omega) \approx H^A(x_c,x_1,\omega)F_c(\omega) + F_{\text{eq}}^T(\omega)\sum_{n=1}^{N} \frac{\varphi_n(x_1)}{m_n[\omega_n^2 - \omega^2 + 2i\omega\omega_n\zeta_n]} \tag{13}$$

$$A_2(\omega) \approx H^A(x_c,x_2,\omega)F_c(\omega) + F_{\text{eq}}^T(\omega)\sum_{n=1}^{N} \frac{\varphi_n(x_2)}{m_n[\omega_n^2 - \omega^2 + 2i\omega\omega_n\zeta_n]} \tag{14}$$

on the basis that, although modal forces $F_n^T(\omega)$ are clearly different – thus, strictly speaking, they cannot be taken out of the summation in Eqs. (13) and (14) – each modal force is essentially effective only within the frequency range of the corresponding tube mode. This assumption should be realistic, provided the modal frequencies are sufficiently separate and the modal damping is low. Then the "equivalent" turbulence force $F_{\text{eq}}^T(\omega)$ stands for *all* modal forces $F_n^T(\omega)$, each one being dominant in the corresponding "modal" frequency range $\omega_n - 0.5\Delta\omega_{n-1} \le \omega \le \omega_n + 0.5\Delta\omega_{n+1}$, where $\Delta\omega_{n-1} \approx \omega_n - \omega_{n-1}$ and $\Delta\omega_{n+1} \approx \omega_{n+1} - \omega_n$.

From the previous discussion, we can write the following formulation to account for the turbulence excitation in an approximate manner:

$$\begin{Bmatrix} F_c(\omega) \\ F_{\text{eq}}^T(\omega) \end{Bmatrix} = \begin{bmatrix} H^A(x_c,x_1,\omega) & G^A(x_1,\omega) \\ H^A(x_c,x_2,\omega) & G^A(x_2,\omega) \end{bmatrix}^{-1} \begin{Bmatrix} A_1(\omega) \\ A_2(\omega) \end{Bmatrix} \tag{15}$$

with each $G^A(x_r,\omega)$ related to turbulence excitation defined as follows:

$$G^A(x_1,\omega) = -\omega^2 \sum_{n=1}^{N} \frac{\varphi_n(x_1)}{m_n[\omega_n^2 - \omega^2 + 2i\omega\omega_n\zeta_n]} \tag{16}$$

$$G^A(x_2,\omega) = -\omega^2 \sum_{n=1}^{N} \frac{\varphi_n(x_2)}{m_n[\omega_n^2 - \omega^2 + 2i\omega\omega_n\zeta_n]} \tag{17}$$

5 Inverse Problem Regularization

The procedure described in Fig. 1 appears deceptively simple. Actually, as for most inverse problems, identification results prove quite sensitive to noise and modeling errors. Regularization methods must be applied when inverting the transfer function $H(x_e,x_r,\omega)$, in order to overcome the perverse effects of the random noise and/or nonmeasured force perturbations. Inversion is most sensitive to noise and unmeasured perturbations in the frequency regions about the antiresonances of the $H(x_e,x_r,\omega)$, which are unduly amplified by the matrix inversion.

Several techniques are available for the regularization of inverse problems. All of them amount to some kind of *filtering*, in order to inhibit the noise amplification, for instance, by applying a form of Tikhonov regularization [29–32], which is both simple to implement and quite effective. However, in the present case, the matrix formulations (5) and (15) lead naturally to the filtering procedure next described. Noise amplification will arise at frequencies where the transformation matrices

$$[M_{(a)}(\omega)] \equiv \begin{bmatrix} H^A(x_c,x_1,\omega) & H^A(x_s,x_1,\omega) \\ H^A(x_c,x_2,\omega) & H^A(x_s,x_2,\omega) \end{bmatrix} \tag{18}$$

or

$$[M_{(b)}(\omega)] \equiv \begin{bmatrix} H^A(x_c,x_1,\omega) & G^A(x_1,\omega) \\ H^A(x_c,x_2,\omega) & G^A(x_2,\omega) \end{bmatrix} \tag{19}$$

are near singular. Among the various techniques which can be used to mitigate the problem, filtering by SVD of $[M(\omega)]$ appears very elegant and effective [29–32]. Singularity of a given matrix can be quantified through the so-called *condition number* $C(\omega)$, which is the ratio between the highest and the lowest singular values of the SVD decomposition

$$[M(\omega)] = [U(\omega)][\Sigma(\omega)][V(\omega)]^T = \sum_{m=1}^{M} \sigma_m(\omega)\{u_m(\omega)\}\{v_m(\omega)\}^T \tag{20}$$

with $\sigma_1 \ge \sigma_2 \ge \ldots \ge 0$. Then, $C(\omega) = \sigma_{\max}/\sigma_{\min} = \sigma_1/\sigma_M$, the matrix being perfectly conditioned when $C=1$ and ill conditioned as C increases. We tend to prefer the use of the inverse quantity $S(\omega) = 1/C(\omega)$ because it nicely normalizes in the range $0 \le S \le 1$, with $S=1$ for perfectly conditioned matrices and $S=0$ for singularity.

The inverse transformation can be computed from the SVD terms as

$$[M(\omega)]^{-1} = [V(\omega)][\Sigma(\omega)]^{-1}[U(\omega)]^T = \sum_{m=1}^{M} \frac{1}{\sigma_m(\omega)}\{v_m(\omega)\}\{u_m(\omega)\}^T \tag{21}$$

and, typically, SVD regularization consists on neglecting all terms such that $S(\omega) < \varepsilon$. Then, Eq. (21) becomes

$$[M^{\text{reg}}(\omega)]^{-1} \approx \sum_{m=1}^{P} \frac{1}{\sigma_m(\omega)}\{v_m(\omega)\}\{u_m(\omega)\}^T \tag{22}$$

with $P \le M$. Actually, because the sensitivities to noise of the acceleration, velocity, and displacement signals are quite different, we have found useful to base the regularization procedure, not on $S(\omega)$, but on the modified quantifier $\hat{S}(\omega)$, see Ref. [33] for a detailed explanation:

$$\hat{S}(\omega) = \frac{\sigma_{\min}(\omega)}{\sigma_M} \quad \text{with} \quad \sigma_M = \max_{0 \le \omega \le \omega_{\max}} [\sigma_{\max}(\omega)] \tag{23}$$

Notice that the definition (23) is less artificial than it seems because such would be the weighing of the (many) singular values obtained if all the spectral terms were assembled in a single large band-matrix, instead of being processed frequency per frequency

$$[M_{\text{TOT}}] \equiv \begin{bmatrix} [M(\omega_1)] & [0] & \cdots & [0] \\ [0] & [M(\omega_2)] & \cdots & [0] \\ \vdots & \vdots & \ddots & \vdots \\ [0] & [0] & \cdots & [M(\omega_{\max})] \end{bmatrix} \tag{24}$$

Inverting $[M_{\text{TOT}}]$ is mathematically equivalent to the inversion of $[M(\omega_1)]$, $[M(\omega_2)]$, etc. However, a straight computation of $S(\omega)$ from (24) would lead to the result $\hat{S}(\omega)$ shown in (23), suggesting why such filtering criterion appears adequate. Note that a direct use of the "assembled" matrix (24), instead of looping on all matrices $[M(\omega)]$ with $0 \le \omega \le \omega_{\max}$, would obviously entail a useless waste of computer resources.

6 Experimental Rig and Test Procedures

Figure 3 shows the actual test rig, which was already sketched in Fig. 2. It consists on a rectangular aluminum beam with cross section 20×10 mm^2 and total length $L=1.267$ m, which is clamped at $x=0$ and free at $x=L$. The beam can only vibrate significantly along its plane of least resistance. An instrumented gap-support is mounted on a micrometric table at location $x_c = 0.682$ m, the contact forces being measured through two piezoelectric force transducers Kistler 9132A with charge amplifiers Kistler 5011. At the gap-supports, the force transducers were fitted with nylon tips, in order to lower the contact stiffness and limit somewhat the high-frequency content of the impacts. Caution partly motivated this decision, in order to restrict the number of

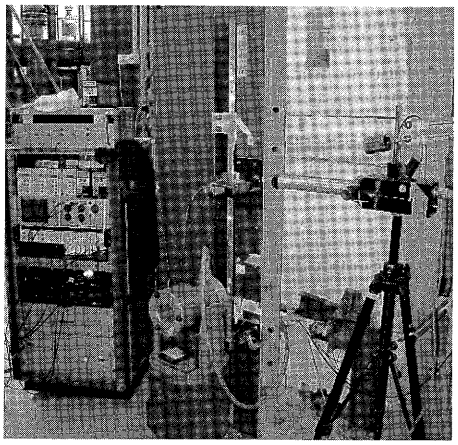

(a)

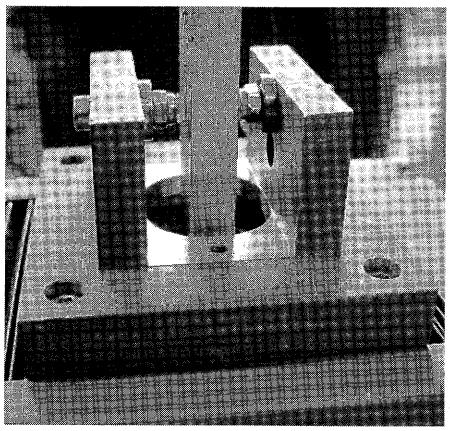

(b)

Fig. 3 Experimental rig. (*a*) General view and (*b*) detail of the instrumented gap-support.

modes excited by the impacts in the present experiments, but on the other side we aimed that a significant part of the impact spectra "melted" with the spectral content of the imposed random excitations.

Experiments have been performed using the following support conditions: (1) a symmetrical support gap of about $\delta_c \approx \pm 0.3$ mm and (2) a "perfect" support with no gaps. As stated before, two different excitation methods have been tested: (a) using an electromagnetic shaker located at $x_s = 0.221$ m, driven by a banded white-noise signal in the range 0–200 Hz, and (b) through the turbulence of a transverse air flow. This random flow excitation was loosely created by impinging on the beam several transverse jets of compressed air, directed along the upper third of the beam, exciting vibration in the lift direction.

Response measurements are provided by two miniature accelerometers Endevco 25A and 2250AM, through charge amplifiers Endevco 2775. These accelerometers, which were used for the identification work, are located, respectively, at $x_1 = 0.4$ m and $x_2 = 1.0$ m. Finally, the beam vibratory displacement near the gap-support was measured using a Zimmer camera OHG-100A. The locations of the loose support and of the measurement transducers were mostly decided for an easy access, as, in practice, the identification technique should be robust enough for most locations. Nevertheless, in order not to degrade the conditioning of transformation matrices (18) and (19), the following cases should be avoided: (a) response transducers located near clamped supports and (b) transducers located too close to each other.

As stated before, identifications are based on the beam unconstrained modes, which are well separated in frequency, as inferred from the preliminary modal identifications. Eight flexural modes proved sufficient for all the identifications performed, ranging from 5.03 Hz up to 788.0 Hz, with modal damping ranging between 0.05% and 0.25%. As an illustration, the transfer functions $H(x_c, x_1, \omega)$ and $H(x_c, x_2, \omega)$ are shown in Fig. 4.

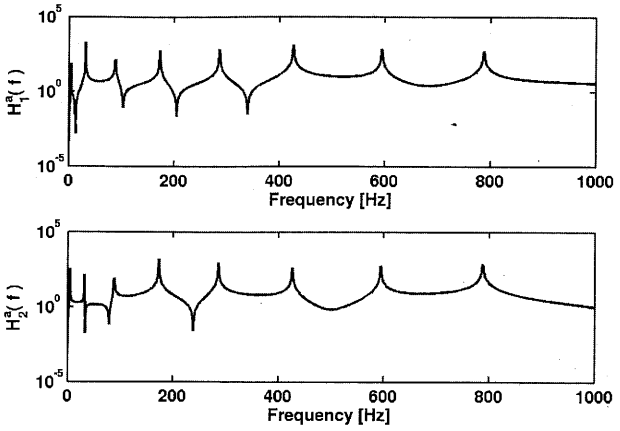

Fig. 4 Transfer functions $H(x_c, x_1, \omega)$ and $H(x_c, x_2, \omega)$ built from the experimentally identified modal parameters

Force identifications have been performed from about 10 s of measured data, using Eq. (5) for the point-excitation or Eq. (15) for the distributed turbulence. Inversion was regularized by using the SVD filtering method, as explained before, with suitable values of the filtering level ε_{opt}, see discussion in Refs. [33,34]. Finally, identification of the beam displacement at the support level was achieved through Eq. (8).

7 Identifications Under Shaker Excitation

Figure 5 shows the two acceleration measurements for the first case, with vibro-impact motion limited by the gap-support. The corresponding auto-spectra are also shown.

The corresponding force identifications are presented in Fig. 6. All identification results presented are zoomed (only 0.4 s are shown), in order to highlight the details of the measured and identified signals. The spiky nature of the impact force and the random shaker excitation forces are both identified in a satisfactory manner. However, the still noticeable background noise could not be squeezed-out of the force identifications without excessive deterioration of the physically meaningful identified signals. The corresponding measured and identified beam vibratory displacement at the gap-support is presented in Fig. 7. The result obtained is also quite satisfactory.

Interesting collateral information is also provided by Fig. 8, where we display the condition number of the matrix transformation $[M_{(a)}(\omega)]$, as a function of frequency, as well as the SVD filtering process, for regularization of the inverse problem. Following the previous discussion, we present in the first plot the condition number $S(\omega) = \sigma_1(\omega)/\sigma_2(\omega)$, as a function of frequency. Then, the second plot shows the corresponding normalized singular values $\hat{S}(\omega) = \sigma_1(\omega)/\sigma_M$ and $\sigma_2(\omega)/\sigma_M$, with $\sigma_M = \max_{0 \le \omega \le \omega_{\max}} [\sigma_2(\omega)]$. Obviously, the condition number $S(\omega)$ significantly decreases when $\hat{S}(\omega)$ decreases, pointing the frequency ranges where the transformation matrices are ill-conditioned. As also shown in the second plot, the information contained in $\hat{S}(\omega)$ allows us to define an adequate level for the SVD truncation, ε_{opt}, such that all information contained in $\sigma_2(\omega)$ are preserved as well as the relevant information in $\sigma_1(\omega)$, while filtering the low singular values at frequencies where the $\sigma_1(\omega)$ are noise-prone. This

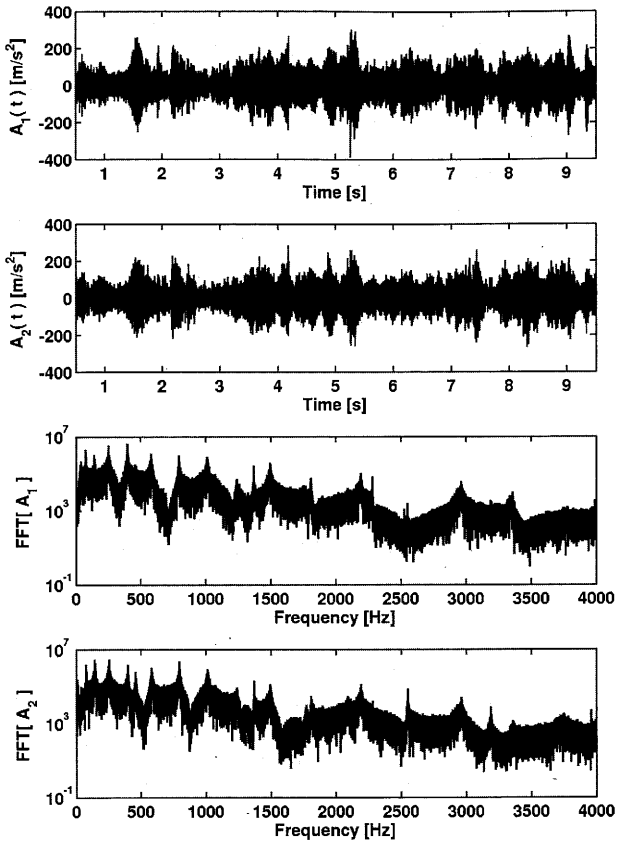

Fig. 5 Acceleration measurements under shaker excitation with a gap-support (time domain and spectra)

is further illustrated in the third plot, where the actual number of singular values (and singular vectors) used for the regularized inversion is shown as a function f frequency.

Next, we present in Figs. 9 and 10 the measured accelerations and force identification results for the no-gap test. Clearly, the results obtained are of very high quality. No data are presented concerning the beam displacement at the non-gap-support, as it is virtually nil.

8 Identifications Under Flow Turbulence

We now turn to the distributed turbulence excitation tests. The measured accelerations, for the case with a gap-support are presented in Fig. 11, as are the corresponding identified impact and excitation forces in Fig. 12. Notice that, now, the identified excitation $F_{eq}^{T}(\omega)$ is not a physical force but an "equivalent" generalized force, as previously discussed.

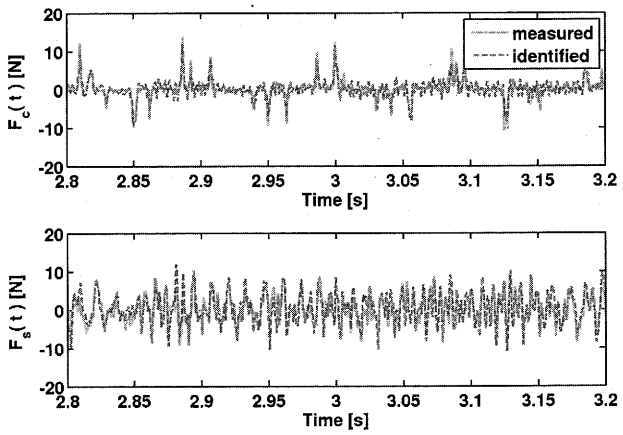

Fig. 6 Shaker excitation with a gap-support. Measured and identified impact force and shaker excitation force.

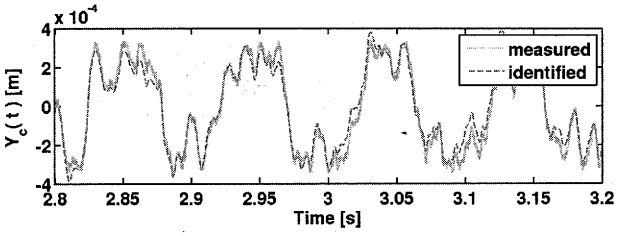

Fig. 7 Shaker excitation with a gap-support. Measured and identified displacement at the gap-support.

Figure 13 displays the measured and identified beam displacements at the gap-support. All these results show a reasonable agreement, suggesting that the approximate technique introduced in Ref. [33] to deal with the distributed flow excitation may indeed be useful in practical applications. As a side point, relevant features related to the condition number, SVD decomposition, and regularization of the transformation matrix $[M_{(b)}(\omega)]$ are presented in Fig. 14.

Finally, we present the identification results for the no-gap configuration under turbulence excitation. The measured responses are shown in Fig. 15 and the identified contact and equivalent generalized excitation forces are shown in Fig. 16. Again, a quite satisfactory impact force identification has been obtained.

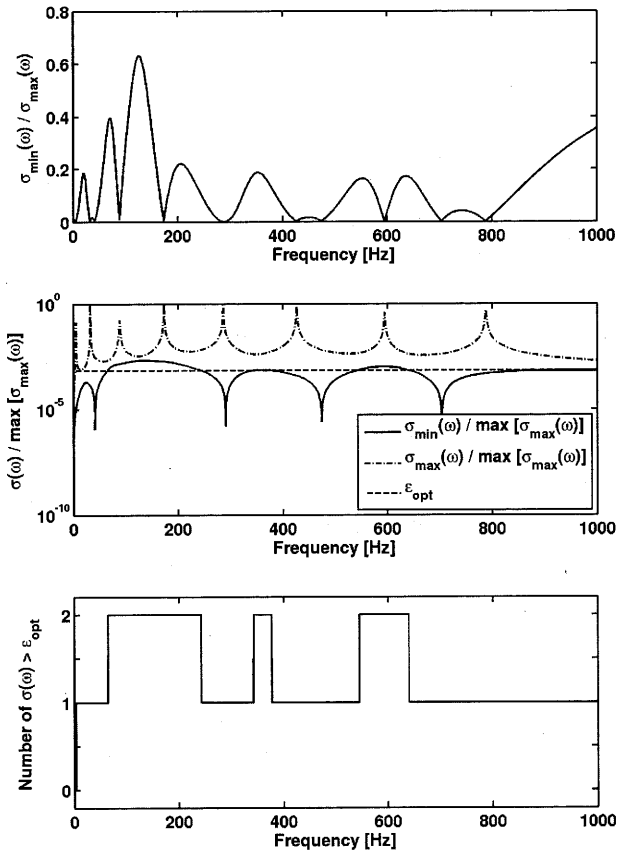

Fig. 8 Condition number of transformation matrix $[M_{(a)}(\omega)]$, SVD decomposition and filtering

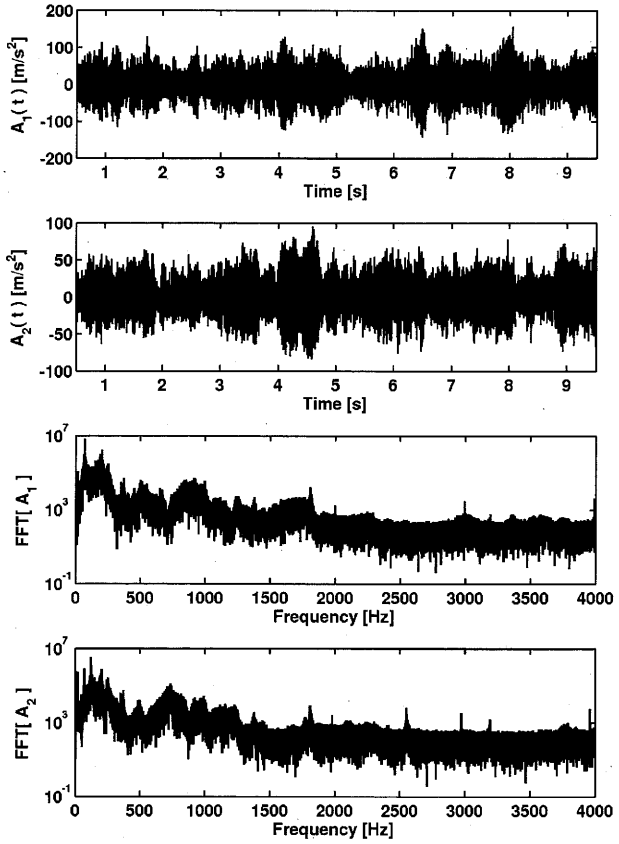

Fig. 9 Acceleration measurements under shaker excitation with a no-gap-support (time domain and spectra)

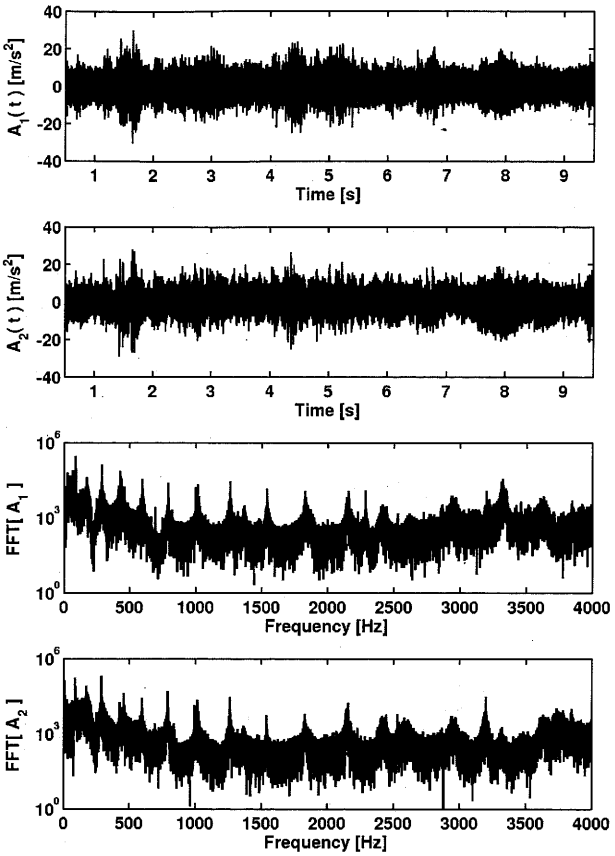

Fig. 11 Acceleration measurements under turbulence excitation with a gap-support (time domain and spectra)

9 Conclusions

In this paper, we have addressed the important topic of remote identification of contact/impact forces motions at gap-supports and preloaded supports. Experimental identifications have been performed on a simple beam subjected to a single nonlinear support, subject to a random point-excitation and also to cross-flow turbulence. Regularization of the inverse problem was achieved using a straightforward SVD filtering method.

Most importantly, using two response measurements, we tested the effectiveness of an approximate identification technique recently introduced [33], which proved effective in minimizing the perturbing effects of the unmeasured distributed turbulence excitation.

The combined use of the various techniques discussed enabled us to achieve experimental identifications of the contact force and of the gap-motions which are of quite acceptable accuracy. Overall, the quality of the identification results ranges from fair to very good, which is encouraging, given the difficulty of the problem. We conjecture that the proposed identification method might work as well for tubes subjected to fluidelastic flow forces. Indeed, these tend to act dominantly on a single low-frequency tube mode, therefore enabling a simpler identification problem.

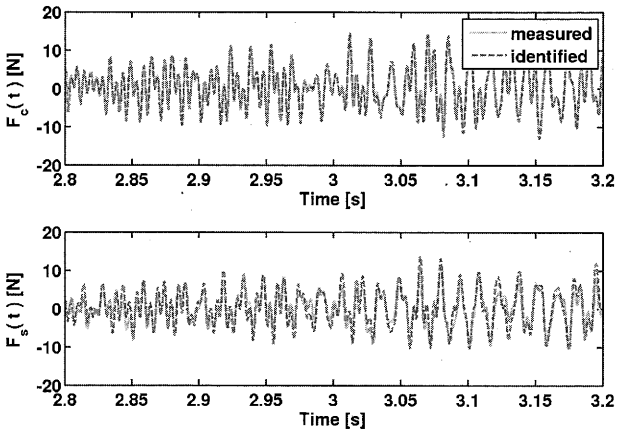

Fig. 10 Shaker excitation with a no-gap-support. Measured and identified impact force and shaker excitation force.

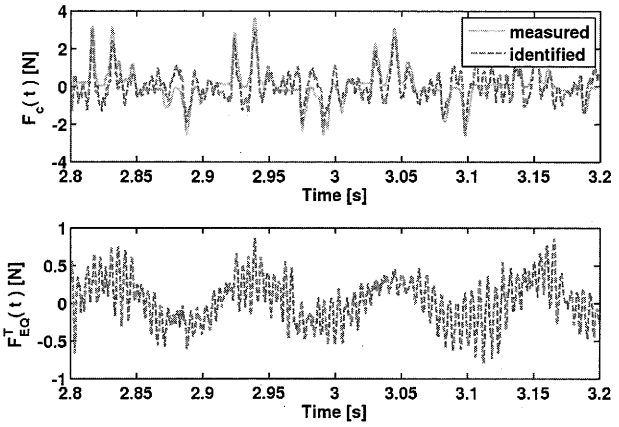

Fig. 12 Turbulence excitation with a gap-support. Measured and identified impact force and equivalent generalized excitation force.

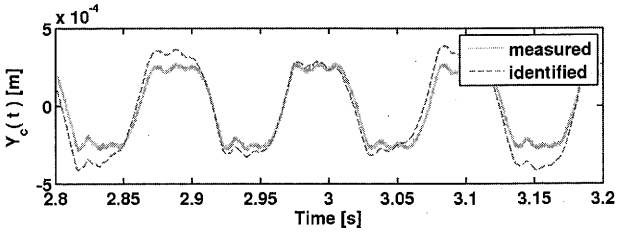

Fig. 13 Turbulence excitation with a gap-support. Measured and identified displacement at the gap-support.

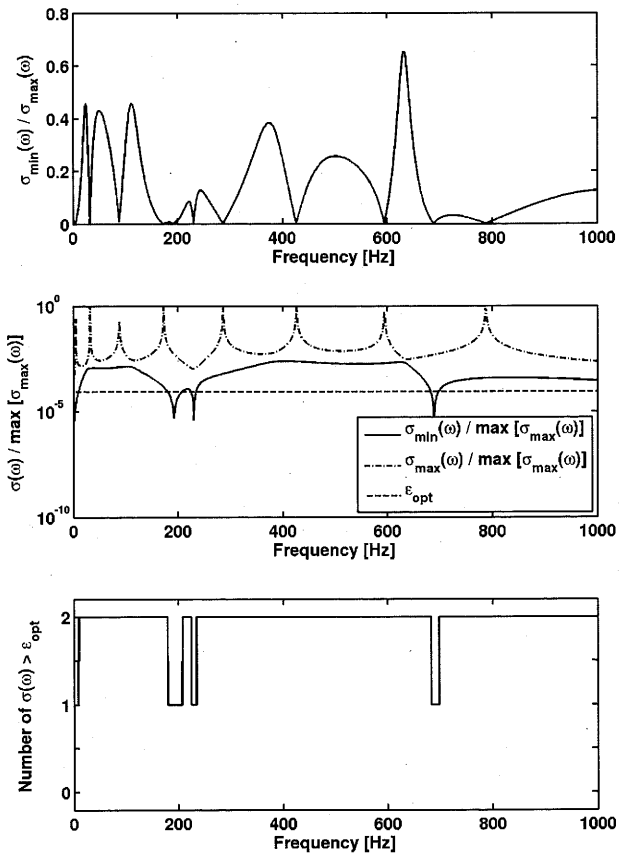

Fig. 14 Condition number of transformation matrix $[M_{(b)}(\omega)]$, SVD decomposition and filtering as a function of frequency

This work should be pursued in the future, in particular by extending these remote identification techniques in order to extract the normal and friction contact forces from three-dimensional beam motions, as well as to cope with multisupported systems. These identification problems will possibly entail new nontrivial difficulties to overcome.

Acknowledgment

Concerning the experimental part of this work, we gladly acknowledge the valuable contribution of Thierry Valin, from CEA/DEN/DM2S/SEMT (Saclay, France). We also thank the constructive comments from anonymous reviewers, which helped to clarify our original manuscript.

Nomenclature

$C(\omega)$ = condition number of the transformation matrix $[M(\omega)]$

$f_c(t) \equiv f(x_c,t)$ = contact/impact force at support x_c

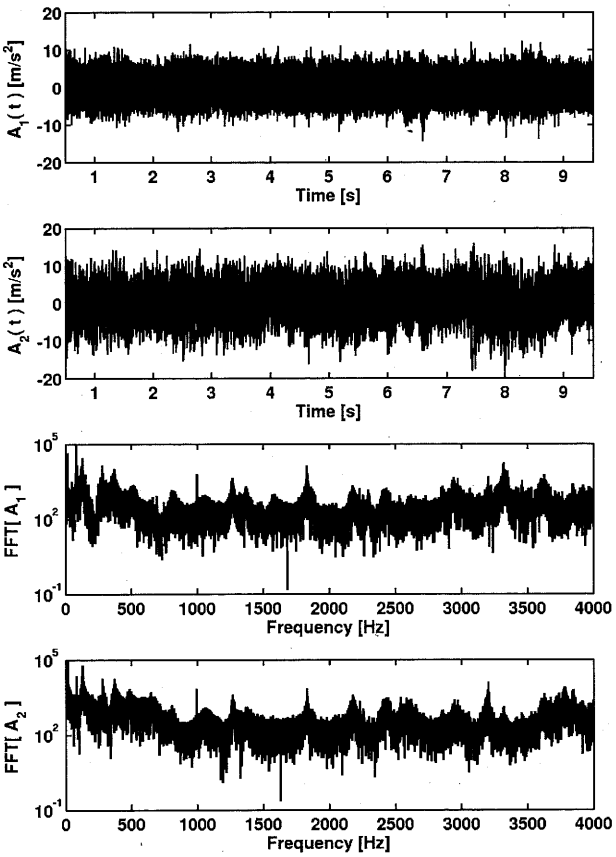

Fig. 15 Acceleration measurements under turbulence excitation with a no-gap-support (time domain and spectra)

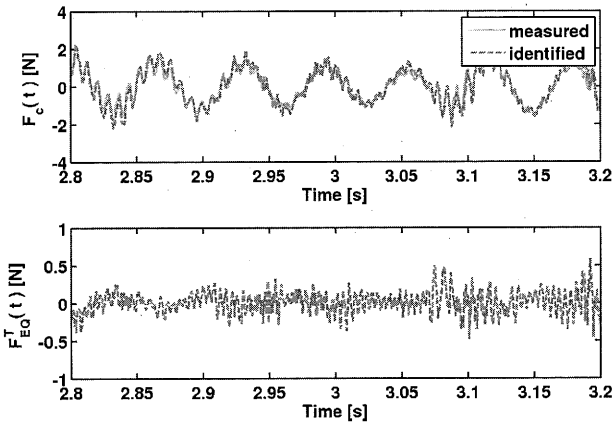

Fig. 16 Turbulence excitation with a no-gap-support. Measured and identified impact force and equivalent generalized excitation force

$F_c(\omega) \equiv F(x_c,\omega)$ = contact/impact force (frequency domain)

$f_n(t)$ = modal force

$F_n(\omega)$ = modal force (frequency domain)

$f_s(t) \equiv f(x_s,t)$ = shaker excitation at location x_s

$F_s(\omega) \equiv F(x_s,\omega)$ = shaker excitation (frequency domain)

$f_T(x,t)$ = distributed turbulence force field

$F_T(x,\omega)$ = distributed turbulence (frequency domain)

$\mathcal{F}[\cdots]$ = Fourier transform

$\mathcal{F}^{-1}[\cdots]$ = inverse Fourier transform

$H(\omega)$ = generic transfer matrix

$[M(\omega)]$ = dynamical transformation matrices
m_n = modal mass
$n=1,2,\ldots,N$ = modal index
$q_n(t)$ = modal response
$S(\omega)=1/C(\omega)$ = modified condition number of the transformation matrix $[M(\omega)]$
t = time
x = axial location
x_c = gap-support location
x_e = excitation location
x_r = response measurement location
x_s = electromagnetic shaker location
$y(x,t)$ = flexural response
δ_c = support gap
ε = SVD truncation level
ω_n = modal circular frequency
ζ_n = modal damping
$\varphi_n(x)$ = mode shape
$u_m(\omega), v_m(\omega)$ = left and right singular vectors of order m as a function of frequency
$\sigma_m(\omega)$ = singular value of order m as a function of frequency
σ_M = maximum of all the singular values $\sigma_m(\omega)$ in the frequency range of interest

References

[1] Rogers, R. J., and Pick, R., 1977, "Factors Associated With Support Forces Due to Heat Exchanger Tube Vibration Contact," Nucl. Eng. Des., **44**, pp. 247–253.
[2] Axisa, F., Antunes, J., and Villard, B., 1988, "Overview of Numerical Methods for Predicting Flow-Induced Vibrations," ASME J. Pressure Vessel Technol., **110**, pp. 7–14.
[3] Antunes, J., Axisa, F., Beaufils, B., and Guilbaud, D., 1990, "Coulomb Friction Modelling in Numerical Simulations of Vibration and Wear Work Rate of Multi-Span Heat-Exchangers," J. Fluids Struct., **4**, pp. 287–304.
[4] Axisa, F., Antunes, J., and Villard, B., 1990, "Random Excitation of Heat-Exchanger Tubes by Cross-Flow," J. Fluids Struct., **4**, pp. 321–341.
[5] Fricker, A., 1991, "Vibro-Impact Behaviour of Fluid-Elastically Unstable Heat Exchanger Tubes With Support Clearances," International Conference on Flow-Induced Vibrations, Proceedings of the Institute of Mechanical Engineers, Brighton, UK, pp. 129–137.
[6] Sauvé, R. G., 1996, "A Computational Time Domain Approach to Fluidelastic Instability for Nonlinear Tube Dynamics," ASME Paper No. PVP-328, pp. 327–335.
[7] Yetisir, M., and Fisher, N., 1996, "Fretting-Wear Prediction in Heat Exchanger Tubes: The Effect of Chemical Cleaning and Modelling Ill-Defined Support Conditions," ASME Paper No. PVP-328, pp. 359–368.
[8] Antunes, J., Axisa, F., and Vento, M., 1992, "Experiments on Tube/Support Interaction With Feedback-Controlled Instability," ASME J. Pressure Vessel Technol., **114**, pp. 23–32.
[9] Boucher, K., and Taylor, C., 1996, "Tube Support Effectiveness and Wear Damage Assessment in the U-Bend Region of Nuclear Steam Generators," ASME Paper No. PVP-328, pp. 285–296.
[10] Fisher, N., Tromp, J., and Smith, B., 1996, "Measurement of Dynamic Interaction Between a Vibrating Fuel Element and Its Support," *ASME Pressure Vessel and Piping Conference*, Montreal, Canada, Paper No. PVP-328, pp. 271–280.
[11] Mureithi, N., Ito, T., and Nakamura, T., 1996, "Identification of Fluidelastic Instability Under Conditions of Turbulence and Nonlinear Tube Supports," ASME Paper No. PVP-328, pp. 19–24.
[12] Vento, M. A., Antunes, J., and Axisa, F., 1992, "Tube/Support Interaction Under Simulated Fluidelastic Instability: Two-Dimensional Experiments and Computations of the Nonlinear Responses of a Straight Tube," ASME Paper No. PVP-242, pp. 151–166.
[13] Whiston, G. S., 1984, "Remote Impact Analysis by Use of Propagated Acceleration Signals, I: Theoretical Methods," J. Sound Vib., **97**, pp. 35–51.
[14] Jordan, R. W., and Whiston, G. S., 1984, "Remote Impact Analysis by Use of Propagated Acceleration Signals, II: Comparison Between Theory and Experiments," J. Sound Vib., **97**, pp. 53–63.
[15] Doyle, J., 1989, *Wave Propagation in Structures: An FFT-Based Spectral Analysis Methodology*, Springer-Verlag, New York.
[16] De Araújo, M., Antunes, J., and Piteau, P., 1998, "Remote Identification of Impact Forces on Loosely Supported Tubes: Part 1—Basic Theory and Experiments," J. Sound Vib., **215**, pp. 1015–1041.
[17] Antunes, J., Paulino, M., and Piteau, P., 1998, "Remote Identification of Impact Forces on Loosely Supported Tubes: Part 2—Complex Vibro-Impact Motions," J. Sound Vib., **215**, pp. 1043–1064.
[18] Paulino, M., Antunes, J., and Izquierdo, P., 1999, "Remote Identification of Impact Forces on Loosely Supported Tubes: Analysis of Multi-Supported Systems," ASME J. Pressure Vessel Technol., **121**, pp. 61–70.
[19] Lin, S. Q., and Bapat, C. N., 1992, "Estimation of Clearances and Impact Forces Using Vibroimpact Response: Sinusoidal Excitation," J. Sound Vib., **157**, pp. 485–513.
[20] Lin, S. Q., and Bapat, C. N., 1993, "Estimation of Clearances and Impact Forces Using Vibroimpact Response: Random Excitation," J. Sound Vib., **163**, pp. 407–421.
[21] Lin, S. Q., and Bapat, C. N., 1993, "Extension of Clearance and Impact Force Estimation Approaches to a Beam-Stop System," J. Sound Vib., **163**, pp. 423–428.
[22] Busby, H. R., and Trujillo, D. M., 1987, "Solution of an Inverse Dynamics Problem Using an Eigenvalue Reduction Technique," Comput. Struct., **25**, pp. 109–117.
[23] Wu, E., and Yeh, J. C., 1994, "Identification of Impact Forces at Multiple Locations on Laminated Plates," AIAA J., **32**, pp. 2433–2439.
[24] Kim, J. T., and Lyon, R. H., 1992, "Cepstral Analysis as a Tool for Robust Processing, Deverberation and Detection of Transients," Mech. Syst. Signal Process., **6**, pp. 1–15.
[25] Antunes, J., Izquierdo, P., and Paulino, M., 2001, "Blind Identification of Impact Forces From Multiple Measurements," Int. J. Nonlinear Sci. Numer. Simul., **2**, pp. 1–20.
[26] Jeffrey, W., and Rosner, R., 1986, "On Strategies for Inverting Remote Sensing Data," Astrophys. J., **310**, pp. 463–472.
[27] Dimri, V., 1992, *Deconvolution and Inverse Theory: Application to Geophysical Problems*, Elsevier, Amsterdam.
[28] Parker, R. L., 1994, *Geophysical Inverse Theory*, Princeton University Press, Princeton, NJ.
[29] Press, W. H., Teukolsky, A. A., Vetterling, W. T., and Flannery, B. P., 1992, *Numerical Recipes: The Art of Scientific Computing*, Cambridge University Press, Cambridge.
[30] Groetch, C. W., 1993, *Inverse Problems in the Mathematical Sciences*, Vieweg & Sohn, Wiesbaden.
[31] Hansen, P. C., 1994, "Regularization Tools," Numer. Algorithms, **6**, pp. 1–35.
[32] Grech, R., Cassar, T., Muscat, J., Camilleri, K., Fabri, S., Zervakis, M., Xanthopoulos, P., Sakkalis, V., and Vanrumste, B., 2008, "Review on Solving the Inverse Problem in EEG Source Analysis," J. Neuroeng. Rehabil., **5**, pp. 579–589.
[33] Delaune, X., Antunes, J., Debut, V., Piteau, P., and Borsoi, L., 2010, "Modal Techniques for Remote Identification of Nonlinear Reactions at Gap-Supported Tubes Under Turbulent Excitation," ASME J. Pressure Vessel Technol., **132**, p. 031801.
[34] Debut, V., Delaune, X., and Antunes, J., 2010, "Identification of the Nonlinear Excitation Force Acting on a Bowed String Using the Dynamical Responses at Remote Locations," Int. J. Mech. Sci., **52**, pp. 1419–1436.